JOURNAL OF SOLID STATE CHEMISTRY 80, 102–111 (1989)

Nonstoichiometry of the Perovskite-Type Oxides $La_{1-x}Sr_xCoO_{3-\delta}$

JUNICHIRO MIZUSAKI,*,† YASUO MIMA,‡ SHIGERU YAMAUCHI,§ AND KAZUO FUEKI‖

Department of Industrial Chemistry, Faculty of Engineering, University of Tokyo, Hongo, Bunkyo-ku, Tokyo 113, Japan

AND HIROAKI TAGAWA

Institute of Environmental Science and Technology, Yokohama National University, 156 Tokiwadai, Hodogaya-ku, Yokohama 240, Japan

Received November 28, 1988

In order to clarify the extent of oxygen nonstoichiometry and defect equilibrium in the oxide solid solution $La_{1-x}Sr_xCoO_{3-\delta}$ (x = 0, 0.1, 0.2, 0.3, 0.5, and 0.7), thermogravimetric measurements were made in the range $10^{-5} \leq P(O_2)/\text{atm} \leq 1$ and $300 \leq T/°C \leq 1000$, where the solid solution was stable as a single-phase perovskite-type oxide. The nonstoichiometry, δ, increases with decreasing $P(O_2)$, increasing Sr content, x, and increasing temperature, T. At temperatures below 800°C, δ of $LaCoO_{3-\delta}$ could not be detected. For $La_{0.3}Sr_{0.7}CoO_{3-\delta}$, a large δ was observed at temperatures as low as 300°C. The observed δ for each $La_{1-x}Sr_xCoO_{3-\delta}$ ranges between 0 and values slightly in excess of $x/2$. Using the Gibbs–Helmholtz equation, the partial molar enthalpy and entropy of oxygen, $(h_O - h_O°)$ and $(s_O - s_O°)$ respectively, were calculated as a function of x and δ. The value of $(h_O - h_O°)$ decreases linearly with increasing δ. The δ dependence of $(s_O - s_O°)$ is determined by the configurational entropy of $V_O^{\cdot\cdot}$ and O_O^x on the oxygen sublattice, while no noticeable contribution was detected from the configurational entropy due to electronic states. This is consistent with the metallic character of the electronic conduction in $La_{1-x}Sr_xCoO_{3-\delta}$.

1. Introduction

The perovskite-type oxide solid solution $La_{1-x}Sr_xCoO_{3-\delta}$ has been of great interest for years as electrode materials for high-temperature fuel cells (*1, 2*), as oxidation and reduction catalysts (*3, 4*), as gas sensor materials (*5, 6*), and as electrode catalysts (*7, 8*). Scientific interest has centered on its high electronic conductivity and magnetic properties which are related to the electronic state of Co-3*d* electrons (*9–11*).

* To whom correspondence should be addressed.

† Present address: Institute of Environmental Science and Technology, Yokohama National University, 156 Tokiwadai, Hodogaya-ku, Yokohama 240 Japan.

‡ Present address: 2nd LSI division, Compound Semiconductor Department, NEC Corp., 1753 Shimonumabe, Nakahara-ku, Kawasaki 211, Japan.

§ Present address: Research Institute, National Rehabilitation Center for Disabled, Namiki, Tokorozawa-shi, Saitama 359, Japan.

‖ Present address: Department of Industrial Chemistry, Science University of Tokyo, Yamazaki, Noda-shi, Chiba 278, Japan.

0022-4596/89 $3.00

The high oxide ion diffusivity (*12, 13*) and the high catalytic activity (*4*) have often been discussed in terms of a large oxygen nonstoichiometry of this material as revealed by studies of $LaCoO_{3-\delta}$ (*14*), $SrCoO_y$ ($2.5 \leq y \leq 3.0$) (*15*), and their solid solutions (*5*). However, because of lack of systematic and precise investigations, the extent of nonstoichiometry, δ, and its relation to temperature, T, Sr content, x, and equilibrium oxygen partial pressure, $P(O_2)$, are not yet clear.

In the present study, the extent of oxygen nonstoichiometry, δ, of the solid solution $La_{1-x}Sr_xCoO_{3-\delta}$ was determined as a function of x, T, and log $P(O_2)$ by means of thermogravimetry and a thermodynamic analysis was carried out to elucidate the defect equilibrium in this solid solution.

2. Experimental

2.1. Sample Preparations

Samples of six compositions, $x = 0$, 0.1, 0.2, 0.3, 0.5, and 0.7 of $La_{1-x}Sr_xCoO_{3-\delta}$, were prepared. The coprecipitation method (*16*) was applied to prepare the samples of $x \leq 0.3$. Aqueous stock solutions of $La(NO_3)_3$, $Sr(NO_3)_2$, and $Co(NO_3)_2$ were prepared by dissolving 99.9% $La_2(CO_3)_3$, $SrCO_3$, and $CoCO_3$, respectively, into aqueous nitric acid. The concentration of each solution was determined by chelatometry using EDTA. The stock solutions were mixed together in appropriate ratios and then poured into a mixture of *n*-butylamine and oxalic acid to precipitate the mixtures of hydroxides and oxalates. The coprecipitate was calcined at 800°C.

A freeze-dry method was applied for the preparation of samples of $x = 0.5$ and 0.7. Each metal carbonate was dissolved into aqueous acetic acid to form the aqueous solution of each metal acetate. These concentrations were analyzed by chelatometry. The solutions were mixed together in a desired ratio and sprayed into liquid nitrogen to form small chilled particles, which were then collected. After freeze-drying, they were heated in vacuum at 180°C to eliminate the residual water and calcined at 400°C.

The calcined materials were ground, baked at 950°C for 30–40 hr in air, and slowly cooled (about 100°C/day). The formation of the perovskite-type single phase was confirmed by X-ray powder analysis. The oxide solid solutions thus obtained were pressed hydrostatically into rods 5 mm in diameter and 10 cm long, sintered at 1000°C in air, and cooled slowly. For samples with $x = 0$ and 0.1, the rods were converted to single crystals by a floating zone technique. The details of the crystal growth are given elsewhere (*16*). A part of the sintered rods or the single crystals (0.6–4 g) was cut and used for thermogravimetry.

2.2. Thermogravimetry

Thermogravimetric measurements were made using an electronic microbalance (Shimazu TG-31H, Cahn type 1000) connected to a reaction tube and a gas flow system. The sample rod was suspended by a platinum wire from an electric microbalance in a silica reaction tube. The reaction tube was placed in a furnace whose temperature was controlled within 0.25°C.

The change with $P(O_2)$ and T in the equilibrium weight due to nonstoichiometry was measured in Ar/O_2 gas mixtures. For the first, the gas mixtures were allowed to flow through a by-pass line to a zirconia oxygen gas sensor to confirm the prepared $P(O_2)$. Then, the gas mixtures were passed through the reaction tube to the zirconia oxygen sensor, and the $P(O_2)$ of outlet gas was monitored.

Equilibrium between the sample and the gas phase was considered to be attained when the following two conditions were satisfied. (i) The weight of the sample reached a constant value. (ii) The $P(O_2)$ of

the gas downstream from the reaction tube became the same to the $P(O_2)$ of the inlet gas. The measurements were made both under the isothermal conditions (i.e., changing $P(O_2)$ stepwise with increasing and decreasing direction) and under iso-$P(O_2)$ conditions (changing temperatures stepwise).

The absolute values of oxygen content in the samples, $x = 0.5$ and 0.7, were measured by reducing the samples in 8% H_2–Ar gas mixtures at 800°C: The samples were annealed at 500°C and slowly cooled (about 100°C/day). Then, the sample (0.6 g) was weighed and placed in the thermogravimetry system, and the temperature was raised to 800°C in air. After evacuation, H_2–Ar gas mixtures were introduced. After reduction by H_2–Ar gas, X-ray powder analysis was made to confirm that the samples, $La_{1-x}Sr_xCoO_{3-\delta}$, had been reduced to the mixtures of La_2O_3, SrO, and Co metal.

Corrections were made for buoyancy of the gas so that the sample weight for each $P(O_2)$ and T was compared by the calculated weight under 1 atm O_2 gas at 298 K. Accuracy in weight measurement after correction for buoyancy was ± 10 μg for the changes in equilibrium weight in O_2–Ar gas mixtures and ± 1 mg for the weight change in the H_2–Ar gas mixtures. In the latter case the accuracy was reduced because of large weight changes.

3. Results and Discussion

3.1. Determination of Nonstoichiometry and Its Temperature Dependence

3.1.1. Temperature dependence of nonstoichiometry in air and in 1 atm O_2 gas. The nonstoichiometry δ of $La_{1-x}Sr_xCoO_{3-\delta}$ is calculated using the equation

$$\delta = (w_O - w_s)M_O/w_O M, \qquad (1)$$

where w_s is the sample weight in equilibrium with appropriate T and $P(O_2)$ conditions, M is the molar weight of oxygen atoms, and w_O and M_O are the weight and the molar weight, respectively, of the sample at the stoichiometric oxygen composition.

For the calculation of δ, we assumed that $La_{1-x}Sr_xCoO_{3-\delta}$ in air has the stoichiometric oxygen composition ($\delta = 0$). We put w_O as the weight of each sample slowly cooled in air from $T > 300$°C. Figure 1 shows the change of equilibrium oxygen content, $3 - \delta$, with temperature, calculated from Eq. (1), in 1 atm of O_2 gas and in air. The above assumption is based both on Wagner's theory (*17*) and on the results of measurements on reduction of samples, as described below.

3.1.2. Determination of stoichiometry by the Wagner theory. According to Wagner (*17*), the slope of δ vs log $P(O_2)$ plot

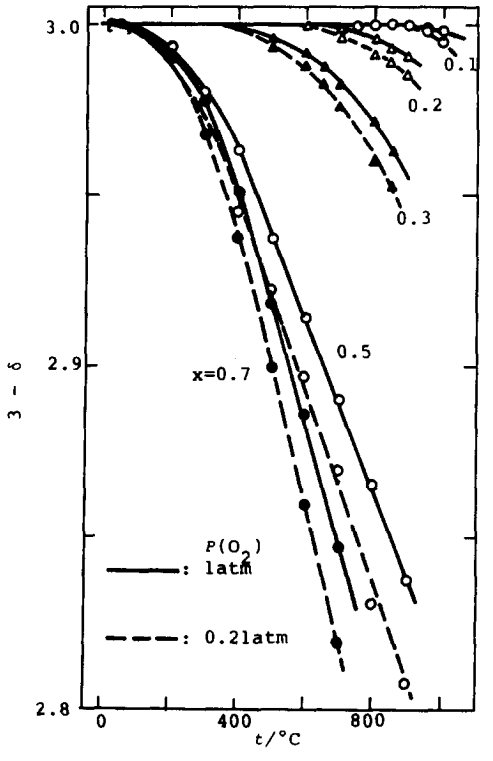

FIG. 1. Temperature change of nonstoichiometry in $La_{1-x}Sr_xCoO_{3-\delta}$ in air and in 1 atm O_2 gas.

($\partial\delta/\partial$ log $P(O_2)$) shows a minimum at the point of its stoichiometric composition.

As shown in Fig. 1, the oxygen content of each sample increases with decreasing temperature. For the samples of $x \leq 0.3$, the oxygen content tends to saturate below 300°C, and the saturated weight in air and in 1 atm oxygen gas are the same. For the samples of $x = 0.5$ and 0.7, the weight increases with decreasing temperature even below 200°C. However, the tendency of weight-saturation is clearly seen, and, at room temperature, the weight in air is the same as that in 1 atm O_2 gas. When the sample is cooled at a rate less than 2–6°C/hr below 200°C, the room temperature weight is reproducible irrespective of the cooling rate. It is concluded that $\partial\delta/\partial$ log $P(O_2)$ is close to 0 near room temperature at $0.2 < P(O_2)/\text{atm} < 1$ atmosphere. Under this condition, according to the Wagner theory (*17*), the samples have composition close to stoichiometry.

For $La_{1-x}Sr_xCoO_{3-\delta}$, no oxygen excess composition has been reported, as any other perovskite-type oxides except for $LaMnO_{3+\delta}$ (*18*). Therefore, it is considered that δ at room temperature in air is close to 0.

3.1.3. Confirmation of stoichiometry by reduction of samples. According to the results of iodometry by Jonker and Van Santen (*19*), the concentration of Co^{4+} in $La_{1-x}Sr_xCoO_{3-\delta}$ is close to that of the Sr content, x, for $x < 0.3$, suggesting that the oxygen content is close to stoichiometry for $x < 0.3$. However, their data showed that the concentration of Co^{4+} tends to saturate with x for $0.3 < x < 0.7$ and decreases with x for $0.7 < x$. This suggests that the samples for $x > 0.3$ used by Jonker and Van Santen were oxygen deficient.

Figure 2 shows typical results of the reduction of $La_{0.5}Sr_{0.5}CoO_{3-\delta}$ and $La_{0.3}Sr_{0.7}CoO_{3-\delta}$. With rising temperature from room temperature to 800°C, the weight

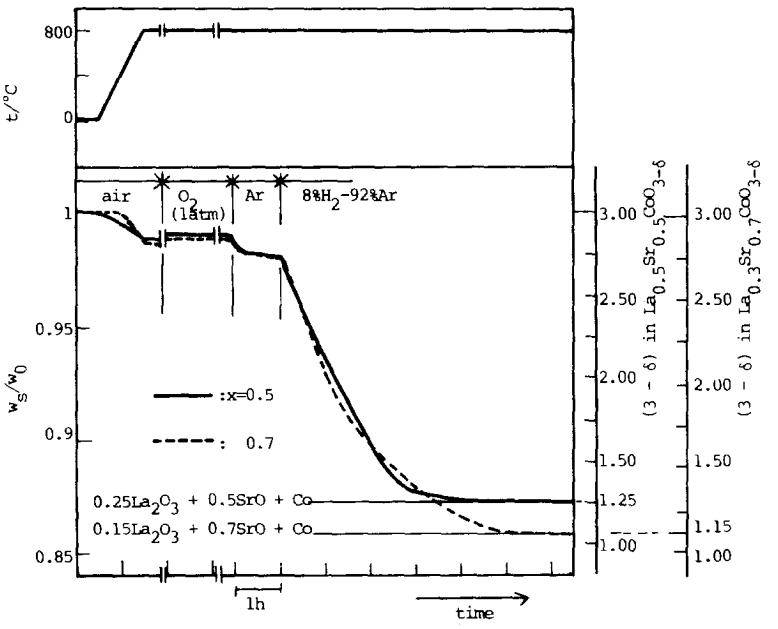

FIG. 2. Results of thermogravimetry for the reduction of $La_{1-x}Sr_xCoO_{3-\delta}$ ($x = 0.5$, 0.7) by 8% H_2–92% Ar gas mixtures. The w_0 is the weight of the sample at room temperature in air.

gradually decreases. When O_2 gas is replaced by Ar gas, the weight changes abruptly. After introducing H_2–Ar gas mixtures, the weight decreases and reaches a stationary value within several hours. X-ray analysis revealed that the samples after reduction were composed of a mixture of La_2O_3, SrO, and Co metal.

Assuming that the reduced sample contains La_2O_3, SrO, and Co in the ratio of 0.25 : 0.5 : 1 for $x = 0.5$ and 0.15 : 0.7 : 1 for $x = 0.7$, the oxygen content, as calculated from the mass change, at room temperature in 1 atm of O_2 was 3.013 ± 0.02 for $x = 0.5$ and 3.020 ± 0.02 for $x = 0.7$. Each value is the average of three runs. The results show that samples for $x = 0.5$ and $x = 0.7$ within experimental error were of stoichiometric composition in air at room temperature.

It is believed that the $\delta = 0$ value also holds in air at room temperature for $x = 0.5$ and $x = 0.7$, provided that the samples were slowly cooled so as to absorb as much oxygen as possible. For the determination of $\delta = 0$, we relied on a theoretical assignment, because the accuracy of gravimetry in the reduction of samples was far below that for equilibrium-weight changes in Ar–O_2 gas mixtures.

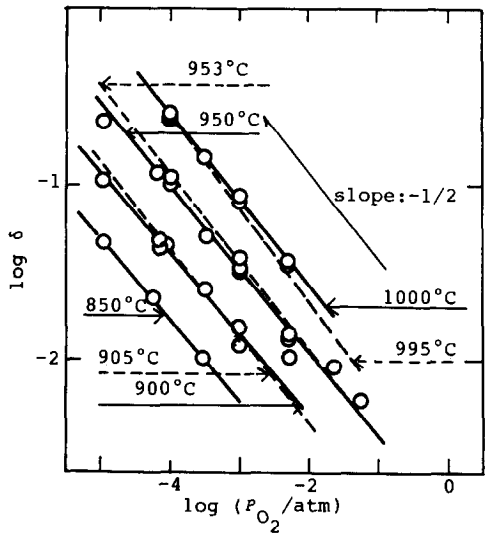

FIG. 3. Nonstoichiometry of $LaCoO_{3-\delta}$ in the log δ vs log $P(O_2)$ plot. The data by Seppänen *et al.* (*14*) are also replotted for comparison.

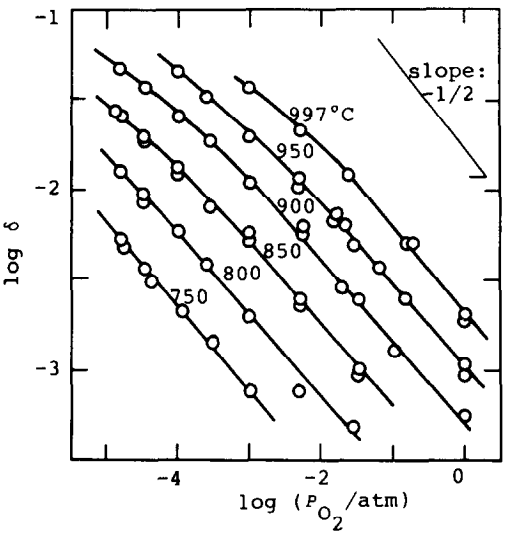

FIG. 4. Nonstoichiometry of $La_{0.9}Sr_{0.1}CoO_{3-\delta}$ in the log δ vs log $P(O_2)$ plot.

3.2 $P(O_2)$ Dependence of δ

Figures 3 and 4 show the nonstoichiometry of $LaCoO_{3-\delta}$ and $La_{0.9}Sr_{0.1}CoO_{3-\delta}$, respectively, in log δ–log $P(O_2)$ plot. (These data were cited in the preceding paper (*20*).) In Fig. 3, the results by Seppänen *et al.* (*14*) based on a coulometric titration method are also shown. The two sets of the data essentially agree with each other.

In Figs. 5 and 6, the nonstoichiometry for $La_{0.7}Sr_{0.3}CoO_{3-\delta}$ and $La_{0.3}Sr_{0.7}CoO_{3-\delta}$ is shown in $(3 - \delta)$ vs log $P(O_2)$ plots. The log δ–log $P(O_2)$ relationships of $La_{1-x}Sr_xCoO_{3-\delta}$ with different Sr content at 800°C are shown in Fig. 7.

The δ value increases with increasing temperature, increasing Sr content, and decreasing $P(O_2)$. The observed δ values range between 0 and $x/2$. As shown in Figs. 3, 4, and 7, for $\delta < 0.01$, δ is almost proportional to $P(O_2)^{-1/2}$. For $\delta > 0.01$, the log $P(O_2)$ dependence of δ becomes weaker

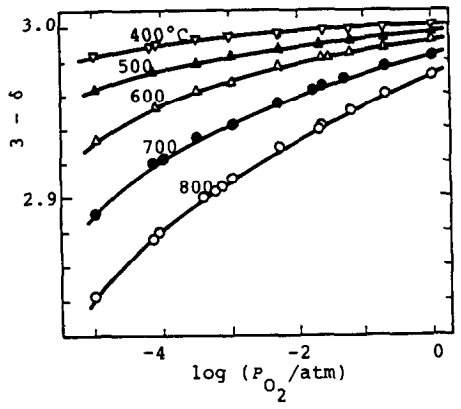

FIG. 5. Nonstoichiometry of $La_{0.7}Sr_{0.3}CoO_{3-\delta}$ as a function of log $P(O_2)$.

with increasing δ. For example, δ of $La_{0.3}Sr_{0.7}CoO_{3-\delta}$ at 800°C varies nearly as the $-1/16$ power of $P(O_2)$.

3.3. Relationship between Mean Co Valence, Nonstoichiometry, and Sr Content

In general, cobalt ions assume valence states between 2+ and 4+, while the valence states of La(3+), Sr(2+), and O(2−) are fixed. Therefore, when a portion, x, of La^{3+} in $LaCoO_3$ is replaced by Sr^{2+} to form $La_{1-x}Sr_xCoO_{3-\delta}$, electroneutrality is maintained by both a decrease in oxygen content and an increase in mean cobalt valence. For $La_{1-x}Sr_xCoO_{3-\delta}$, the mean cobalt valence, n, is given by

$$n = 3 + x - 2\delta. \tag{2}$$

From the nonstoichiometry data in Figs. 1 and 3–7, the oxygen content, $3 - \delta$, and the mean cobalt valence, n, are calculated as a function of x at each temperature and $P(O_2)$. Figure 8 shows the relationships at 800°C. For $x \leq 0.2$, the increase in x results mainly in an increase of the mean Co valence. For $0.2 < x < 0.5$, the increase in x mainly contributes to an increase in δ. For $x > 0.5$, the increase in x again results in the

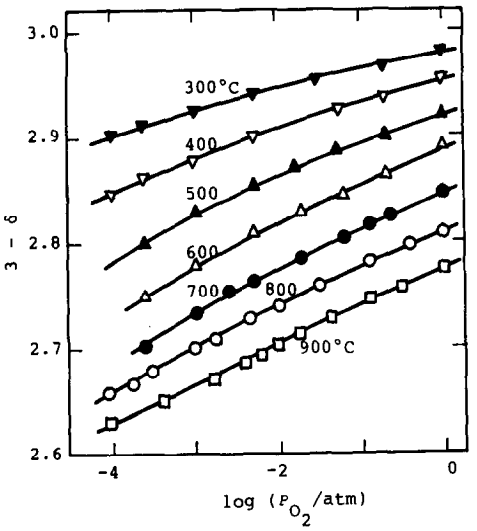

FIG. 6. Nonstoichiometry of $La_{0.3}Sr_{0.7}CoO_{3-\delta}$ as a function of log $P(O_2)$.

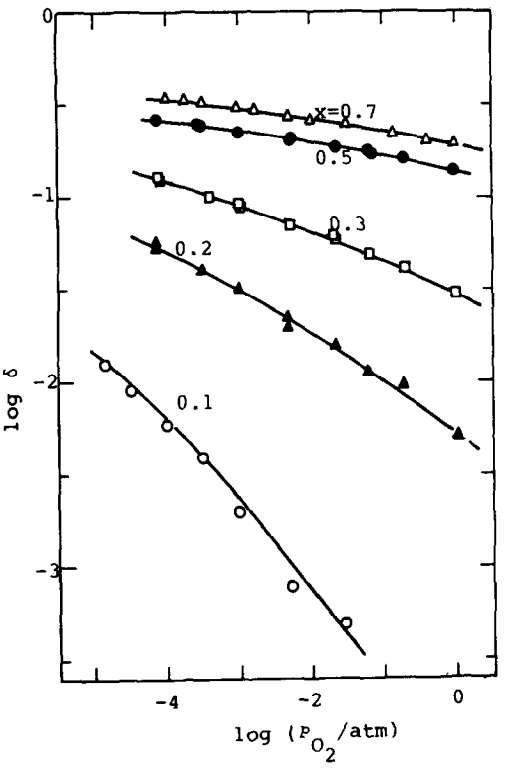

FIG. 7. Log δ vs log $P(O_2)$ plots of $La_{1-x}Sr_xCoO_{3-\delta}$ with different Sr content at 800°C.

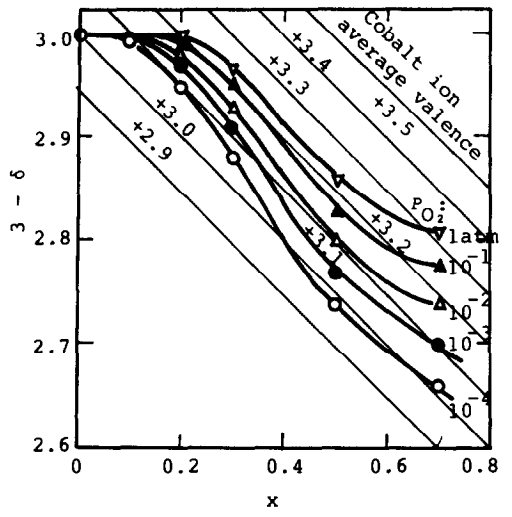

FIG. 8. Change of oxygen content and mean cobalt valence with Sr content in $La_{1-x}Sr_xCoO_{3-\delta}$ at 800°C.

increase in mean cobalt valence. The similar tendency is also observed at other temperatures.

3.4. $P(O_2)$ Dependence of δ as Compared with other Perovskite-Type Oxides

The thermodynamic data of $La_{1-x}Sr_xMO_{3-\delta}$ (M = Cr, Fe, and Co) are compared (*21, 22*) in Fig. 9. The $(3 - \delta)$ vs log $P(O_2)$ plots for $La_{1-x}Sr_xCrO_{3-\delta}$ and $La_{1-x}Sr_xFeO_{3-\delta}$ show inflection points at $\delta = x/4$ and plateaus at $\delta = x/2$, while the plots for $La_{1-x}Sr_xCoO_{3-\delta}$ show neither an inflection point nor a plateau.

The plateau at $\delta = x/2$ is generally attributed to "electronic stoichiometry" in the compound. Here, the average valence of M ions in $La_{1-x}Sr_xMO_{3-\delta}$ is 3+. For the cases of $La_{1-x}Sr_xCrO_{3-\delta}$ (*21*) and $La_{1-x}Sr_xFeO_{3-\delta}$ (*23*), the electrons are considered to be strongly localized on Cr or Fe ions. The plateau represents the stoichiometry condition

$$[M_M^{\cdot}] = [M_M^{\prime}]. \qquad (3)$$

It is known (*24*) that the plateau at $\delta = x/2$ may also appear if $La_{1-x}Sr_xMO_{3-\delta}$ is a wide-band gap semiconductor and the M^{3+} state corresponds a filled band state. In this case, $n = p$ holds at $\delta = x/2$.

For $La_{1-x}Sr_xCoO_{3-\delta}$, in contrast to $La_{1-x}Sr_xFeO_{3-\delta}$ and $La_{1-x}Sr_xCrO_{3-\delta}$, no plateau appears at $\delta = x/2$. This fact indicates that the electrons are not strongly localized on Co ions; also, $La_{1-x}Sr_xCoO_{3-\delta}$ is not a wide-band gap semiconductor with a filled valence band at $\delta = x/2$. Therefore, $La_{1-x}Sr_xCoO_{3-\delta}$ may have a metallic or semimetallic electronic state at the temperatures of our measurements.

This result largely agrees with earlier band models proposed based on electronic and magnetic measurements (*1, 10, 15*).

3.5. Partial Molar Quantities

The chemical potential, μ_O, of $La_{1-x}Sr_xCoO_{3-\delta}$ in equilibrium with gas at an oxygen partial pressure $P(O_2)$ (atm) can be expressed by

$$\mu_O - \mu_O^\circ = (RT/2) \ln P(O_2), \qquad (4)$$

where μ_O° denotes μ_O values of $La_{1-x}Sr_xCoO_{3-\delta}$ in equilibrium with 1 atm O_2 (g).

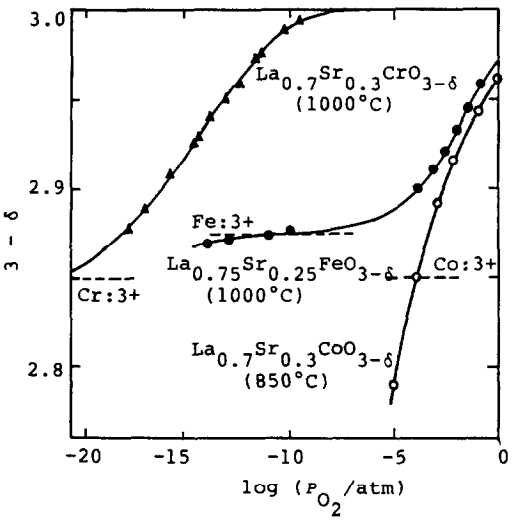

FIG. 9. Comparison of nonstoichiometry data of $La_{1-x}Sr_xMO_{3-\delta}$ (M = Cr, Fe, Co).

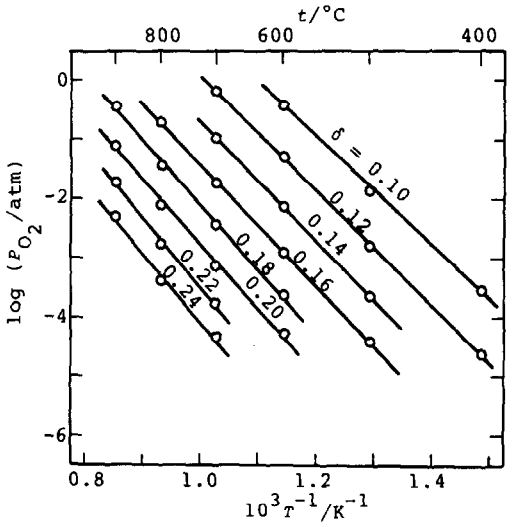

FIG. 10. Nonstoichiometry of $La_{0.5}Sr_{0.5}CoO_{3-\delta}$ in the log $P(O_2)$ vs $1/T$ plot with δ as a parameter.

Defining the partial molar enthalpy as h_O and the partial molar entropy as s_O for oxygen in $La_{1-x}Sr_xCoO_{3-\delta}$, μ_O can be expressed by the equation

$$\mu_O = h_O - Ts_O. \quad (5)$$

From Eqs. (4) and (5), we obtain the relationships

$$h_O - h_O^\circ = (R/2)[\partial \ln P(O_2)/\partial(1/T)] \quad (6)$$

and

$$s_O - s_O^\circ = -(1/2)[\partial(RT \ln P(O_2))/\partial T], \quad (7)$$

where h_O° and s_O° are h_O and s_O, respectively, of $La_{1-x}Sr_xCoO_{3-\delta}$ in equilibrium with 1 atm $O_2(g)$.

Figure 10 shows a plot of log $P(O_2)$ vs $1/T$ for $La_{0.5}Sr_{0.5}CoO_{3-\delta}$. From the slope of the plots, using Eq. (6), $(h_O - h_O^\circ)$ can be determined. The plots for all $La_{1-x}Sr_xCoO_{3-\delta}$ form straight lines. Therefore, $(h_O - h_O^\circ)$ for each δ is essentially independent of temperature. The $(h_O - h_O^\circ)$ values are shown in Fig. 11 as a function of δ.

Using Eq. (7), the $(s_O - s_O^\circ)$ values can be determined from the slopes of the $RT \ln P(O_2)$ vs T plots. The plots for all $La_{1-x}Sr_xCoO_{3-\delta}$ also form straight lines. Therefore, $(s_O - s_O^\circ)$ values are also essentially independent of T. The calculated $(s_O - s_O^\circ)$ values are shown in Fig. 12.

As shown in Fig. 11, $(h_O - h_O^\circ)$ changes almost linearly with δ, as expressed by

$$h_O - h_O^\circ = \Delta h_O^\circ(x) - a\delta. \quad (8)$$

The values of $\Delta h_O^\circ(x)$ and a are shown in Fig. 13.

Because changes of oxygen concentration in $La_{1-x}Sr_xCoO_{3-\delta}$ result in changes of

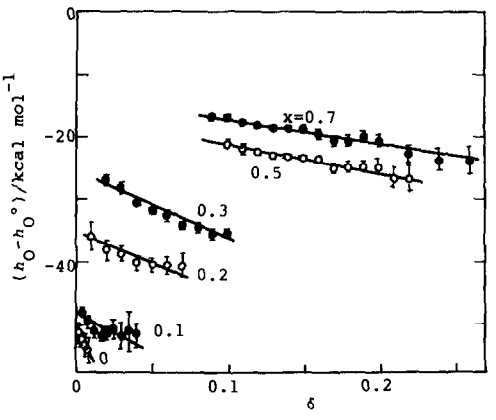

FIG. 11. Oxygen partial molar enthalpy of $La_{1-x}Sr_xCoO_{3-\delta}$ as a function of δ for different Sr content.

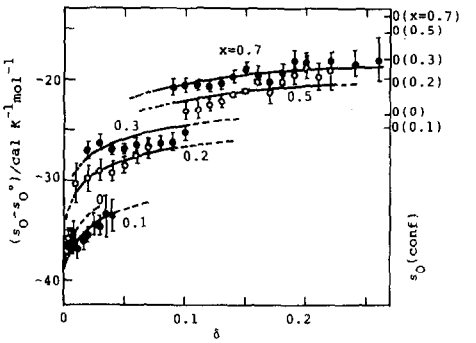

FIG. 12. Oxygen partial molar entropy of $La_{1-x}Sr_xCoO_{3-\delta}$ as a function of δ for different Sr content. Solid curves are the fitting ones to Eq. (13). On the right-hand scale, the points of s_O(conf) = 0 for respective Sr contents are indicated.

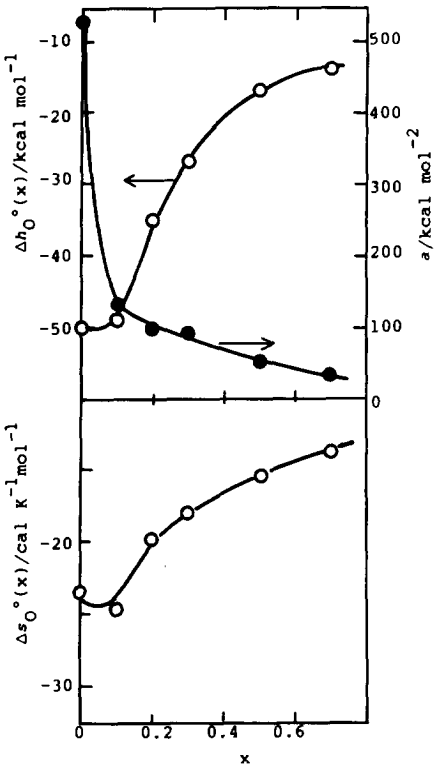

FIG. 13. Plots of $\Delta h_O°(x)$, a, and $\Delta s_O°(x)$ as a function of x.

mean oxide ion vacancy concentration and of mean cobalt valence, s_O includes the partial molar entropies of the configurational entropy change of oxygen lattice sites, s_O(conf), and the entropy change of the electronic state of cobalt $3d$ orbital (or $3d$ band), s_O(elec).

If the oxide ion vacancies are randomly distributed on the oxygen sublattice, s_O(conf) can be expressed by

$$s_O(\text{conf}) = k(\partial/\partial N_O)\ \ln(N!/N_O!N_V!); \quad N = N_O + N_V, \quad (9)$$

where N, N_O, and N_V are the numbers of oxygen lattice sites, oxygen atoms, and oxide-ion vacancies, respectively. For 1 mole of $La_{1-x}Sr_xCoO_{3-\delta}$, we have

$$N = 3A_v, \quad (10)$$

$$N_O = (3 - \delta)A_v \quad (11)$$

and

$$N_v = \delta A_v, \quad (12)$$

where A_v is the Avogardo constant.

Using Eqs. (9)–(12), we obtain

$$s_O(\text{conf}) = R\ \ln(\delta/(3 - \delta)). \quad (13)$$

The solid curves in Fig. 12 represent the fits to Eq. (13). The point s_O(conf) = 0 given for each composition is shown in the right-hand-side scale. The fitting curves essentially agree with the calculated s_O values. Therefore, it is concluded that the change of $(s_O - s_O°)$ with δ is approximately expressed by the equation

$$s_O - s_O° = \Delta s_O°(x) + s_O(\text{conf}), \quad (14)$$

where $\Delta s_O°(x)$ is a constant. The $\Delta s_O°(x)$ values are shown in Fig. 13.

Because the change with δ of s_O is determined by s_O(conf), given in Eq. (13), the random distribution approximation holds for the distribution of oxygen vacancies in $La_{1-x}Sr_xCoO_{3-\delta}$. Since s_O(elec), the entropy change of $3d$ electronic state with δ, is found to be very small, the change with δ of the $3d$ electronic state is considered to be very small. This suggests that the electronic state of $La_{1-x}Sr_xCoO_{3-\delta}$ is metallic or semimetallic, as already indicated in Section 3.4.

Acknowledgment

The authors gratefully acknowledge Mr. Yuuji Kuwayama, undergraduate student of Yokohama National University, for his help in the thermogravimetric determination of oxygen content in the samples.

References

1. J. B. GOODENOUGH AND R. C. RACCAH, *J. Appl. Phys.* **36,** 1031 (1963).
2. Y. OHNO, S. NAGATA, AND H. SATO, *Solid State Ionics* **3/4,** 439 (1981).
3. M. W. CHIEN, I. M. PEARSON, AND K. NOBE, *Ind. Eng. Chem. Prod. Res. Dev.* **14,** 131 (1975).

4. T. NAKAMURA, M. MISONO, AND Y. YONEDA, *Chem. Lett.*, 1589 (1981).
5. H. OBAYASHI AND T. KUDO, "Application of Solid Electrolytes," p. 102, JEC Press, Cleveland, OH (1980).
6. Y. YAMAMURA, Y. NINOMIYA, AND S. SEKIDO, "Proceedings of the International Meeting on Chemical Sensors" (T. Seiyama *et al.*, Eds.), p. 187, Kodansha/Elsevier, Tokyo/Amsterdam (1983).
7. J. O'M. BOCKRIS AND T. OTAGAWA, *J. Electrochem. Soc.* **131,** 290 (1984).
8. J. VONDRAK AND L. DOLEZAL, *Electrochim. Acta* **29,** 477 (1984).
9. G. H. JONKER, *Phillips Res. Rep.* **24,** 1 (1969).
10. P. M. RACCAH AND J. B. GOODENOUGH, *J. Appl. Phys.* **39,** 1209 (1968).
11. H. TAGUCHI, M. SHIMADA, AND M. KOIZUMI, *Mater. Res. Bull.* **13,** 1225 (1978).
12. A. G. C. KOBUNSSEN, F. R. VAN BÜREN, AND G. H. J. BROERS, *J. Electroanal. Chem.* **91,** 211 (1978).
13. T. ISHIGAKI, S. YAMAUCHI, J. MIZUSAKI, K. FUEKI, AND H. TAMURA, *J. Solid State Chem.* **54,** 100 (1984).
14. M. SEPPÄNEN, M. KYTO, AND P. TASKINEN, *J. Metall.* **9,** 3 (1980).
15. H. TAGUCHI, M. SHIMADA, AND M. KOIZUMI, *J. Solid State Chem.* **29,** 221 (1979).
16. T. MATSUURA, T. ISHIGAKI, J. MIZUSAKI, S. YAMAUCHI, AND K. FUEKI, *Japan. J. Appl. Phys.* **23,** 1172 (1984).
17. C. WAGNER, *Proc. Solid State Chem.* **6,** 1 (1971).
18. T. NAKAMURA, G. PETZOW, AND L. J. GAUCKLER, *Mater. Res. Bull.* **14,** 649 (1979).
19. G. H. JONKER AND J. H. VAN SANTEN, *Physica* **19,** 120 (1953).
20. K. FUEKI, J. MIZUSAKI, S. YAMAUCHI, T. ISHIGAKI, AND Y. MIMA, *Mater. Sci. Monogr.* **28**(A), 339 (1985).
21. J. MIZUSAKI, S. YAMAUCHI, K. FUEKI, AND A. ISHIKAWA, *Solid State Ionics* **12,** 119 (1984).
22. J. MIZUSAKI, M. YOSHIHIRO, S. YAMAUCHI, AND K. FUEKI, *J. Solid State Chem.* **58,** 257 (1985).
23. J. MIZUSAKI, T. SASAMOTO, W. R. CANNON, AND H. K. BOWEN, *J. Amer. Ceram. Soc.* **66,** 247 (1983).
24. F. A. KRÖGER, "Chemistry of Imperfect Crystals," North-Holland, New York (1974).